

Ruthenium(II)–Arene RAPTA Type Complexes Containing Curcumin and Bisdemethoxycurcumin Display Potent and Selective Anticancer Activity

Riccardo Pettinari,^{*,†} Fabio Marchetti,[‡] Francesca Condello,[†] Claudio Pettinari,[†] Giulio Lupidi,[†] Rosario Scopelliti,[§] Suman Mukhopadhyay,[§] Tina Riedel,[§] and Paul J. Dyson^{*,§}

[†]School of Pharmacy and [‡]School of Science and Technology, University of Camerino, via S. Agostino 1, 62032 Camerino MC, Italy

[§]Institut des Sciences et Ingénierie Chimiques, Ecole Polytechnique Fédérale de Lausanne (EPFL), 1015 Lausanne, Switzerland

Supporting Information

ABSTRACT: A series of novel ruthenium(II) arene RAPTA type derivatives (arene = cymene, hexamethylbenzene) containing curcumin-based ligands (curcH = curcumin, bdcurch = bisdemethoxycurcumin) and PTA (1,3,5-triaza-7-phosphaadamantane) have been synthesized and fully characterized. The solid-state structures of [Ru(cym)(curc)-(PTA)][SO₃CF₃], [Ru(hmb)(curc)(PTA)][SO₃CF₃], and [Ru(hmb)(bdcurch)(PTA)][SO₃CF₃] have been determined by single-crystal X-ray diffraction. The antitumor activity of the complexes has been evaluated in vitro against human ovarian carcinoma cells (A2780 and A2780cisR), as well as against nontumorous human embryonic kidney (HEK293) cells. The correlation of the cytotoxicity upon switching the curcumin-based ligands, i.e. curcumin vs bisdemethoxycurcumin, is not straightforward. In contrast, the PTA ligand greatly enhances the activity and selectivity of ruthenium compounds in comparison to previously reported compounds.

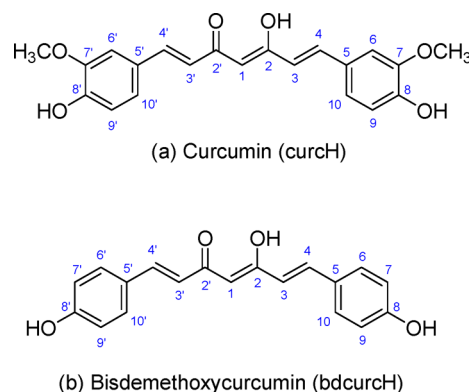


INTRODUCTION

Platinum-based drugs are extensively used in the clinic to treat many types of cancers.¹ However, their application is limited by severe side effects and drug resistance, and consequently complexes based on other metal ions have attracted attention.² In this regard ruthenium-based compounds are among the most promising, with two ruthenium(III) complexes undergoing clinical evaluation.³ Organometallic ruthenium(II) arene complexes also exhibit promising pharmacological properties.⁴ The relatively robust nature of ruthenium(II) arene complexes allows their rational modification such that an organic compound of known therapeutic value may be tethered to the motif. This type of modification has been achieved via covalent binding of the functional organic moiety to the arene⁵ or via one of the other ligands.⁶ Direct coordination of the organic moiety, i.e. using it as a ligand, represents another approach, and in this context ruthenium(II) arene complexes have been derivatized with curcumin.⁷ Curcumin is a low-molecular-weight polyphenol (Scheme 1a) and is the major bioactive ingredient extracted from the rhizome of the plant *Curcuma longa* (turmeric)⁸ that has a number of relevant medicinal properties.⁹ Since curcumin possesses anti-inflammatory, antioxidant, and antitumoral effects, it has been extensively studied as a chemopreventive agent in some cancer models and used in the therapeutic selection in clinical oncology. However, curcumin is insoluble and unstable in water.

As a continuation of previous works,⁷ water-soluble ruthenium(II) arene compounds with curcumin-based ligands were synthesized. Despite the fact that these compounds

Scheme 1. Structures of the Proligands Employed Herein



displayed reasonable properties in vitro, we decided to replace the chloride ligand with a 1,3,5-triaza-7-phosphaadamantane ligand. Simple ruthenium(II) arene complexes with a PTA ligand display antimetastatic activity in vivo,¹⁰ as well as an intrinsic antiangiogenic activity¹¹ and the ability to reduce the growth of certain primary tumors.¹²

Herein we report novel derivatives containing both PTA and curcuminoid ligands, their full solution and solid-state characterization, and the study of their antiproliferative effect

Received: March 24, 2014

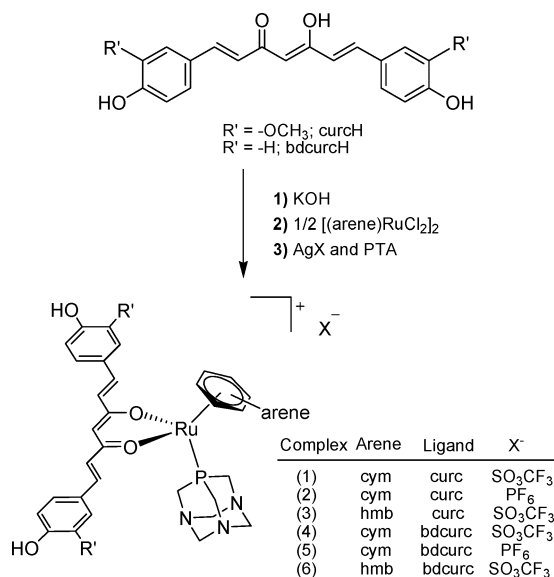
Published: July 15, 2014

against human ovarian carcinoma cells relative to nontumorous human embryonic kidney cells.

RESULTS AND DISCUSSION

Synthesis and Characterization of Ruthenium Complexes. The desired ruthenium(II) arene complexes **1–6** were prepared in high yield in a single step (Scheme 2), in which the substitution of chloride ligand with PTA in the ruthenium coordination environment is achieved by applying silver salts, i.e. AgX, where X = SO₃CF₃, PF₆.

Scheme 2. Synthesis of Complexes **1–6**



Complexes **1–6** are air stable and soluble in alcohols, acetone, acetonitrile, and DMSO and slightly soluble in chlorinated solvents. The IR spectra of **2** and **5** display a strong, sharp absorption at 825 and 826 cm⁻¹ due to the PF₆ counteranion,¹³ whereas the spectra of **1**, **3**, **4**, and **6** contain a characteristic absorption pattern in the region 1000–1200 cm⁻¹, typical of a noncoordinated O₃SCF₃ anion.¹⁴ The ¹H NMR spectra of **1–6** display all the expected signals due to the coordinated arene rings, curc or bdcH ligand, and PTA. The resonances due to the PTA ligand are shifted to lower field with respect to those of uncoordinated PTA, confirming its coordination to the ruthenium center.¹⁵ The ³¹P NMR spectra of **1**, **2**, **4**, and **5**, containing the *p*-cymene moiety, display a singlet centered at ca. -26 ppm, whereas **3** and **6** with the hexamethyl moiety show a resonance at -32 ppm, in the range typical of related compounds and in accordance with the existence of only one species in solution.¹⁶ The ESI mass spectra of **1–6** show two main peak envelopes, that of highest relative intensity corresponding to the intact [Ru(arene)(curc/bdcH)(PTA)]⁺ species and the other being due to the [Ru(arene)(curc/bdcH)]⁺ fragment formed upon PTA dissociation.

The solid-state structures of **1**, **3**, and **6** were established by X-ray crystallography (see the Experimental Section). Their structures are shown in Figure 1, and principal bond parameters are given in the caption. The bond lengths are essentially typical values, although the O1–Ru1–O2 bond angles are 89.13(6), 87.78(7), and 87.9(2)° for **1**, **3**, and **6**, respectively, indicating that the six-membered metallacycle is less strained

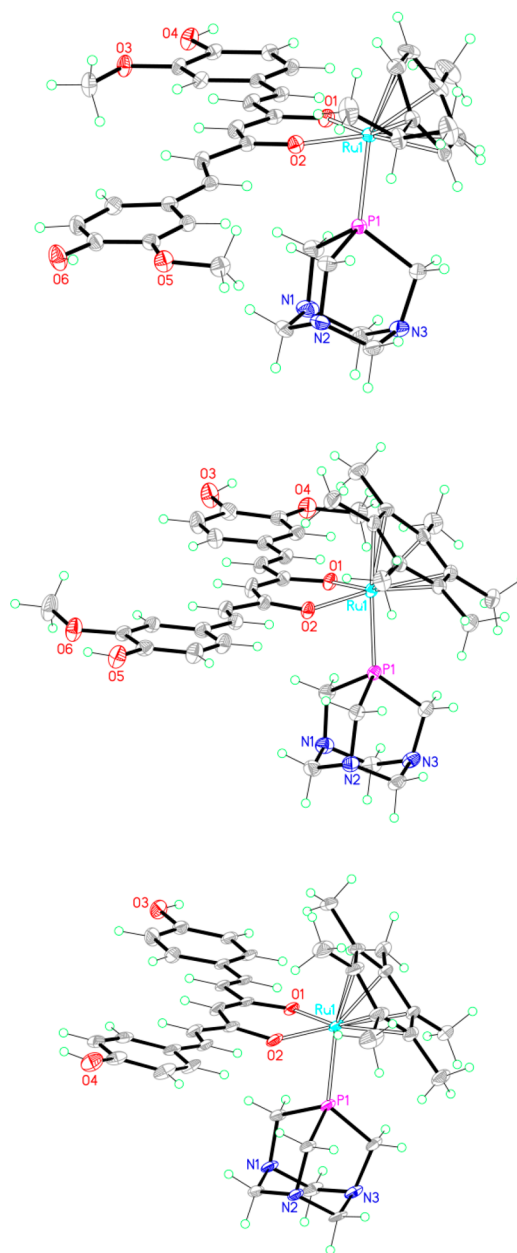


Figure 1. Molecular structures of **1** (top), **3** (middle), and **6** (bottom). Counterions and solvates have been omitted for clarity. Selected bond lengths (Å) and angles (deg) for **1**: Ru1–O2, 2.082(2); Ru1–O1, 2.089(2); Ru1–P1, 2.308(1); Ru1– η^6 , 1.713(1); O1–Ru1–O2, 89.13(6); P1–Ru1–O2, 83.43(5); P1–Ru1–O1, 88.89(5). Selected bond lengths (Å) and angles (deg) for **3**: Ru1–O2, 2.080(2); Ru1–O1, 2.092(2); Ru1–P1, 2.324(1); Ru1– η^6 , 1.702(1); O1–Ru1–O2, 87.78(7); P1–Ru1–O2, 82.07(5); P1–Ru1–O1, 87.88(5). Selected bond lengths (Å) and angles (deg) for **6**: Ru1–O2, 2.086(6); Ru1–O1, 2.091(5); Ru1–P1, 2.328(2); Ru1– η^6 , 1.707(6); O1–Ru1–O2, 87.9(2); P1–Ru1–O2, 83.2(2); P1–Ru1–O1, 86.9(2).

than that observed in [Ru(η^6 -cym)(PTA)(C₂O₄)] (O1–Ru1–O2 = 78.43(7)°),¹⁷ but is in keeping with the equivalent angles in related complexes.¹⁸ In comparison, the two chloride ligands coordinated to RAPTA-C are displaced at a bond angle of 89.16(4)°.¹⁹

The stability of **1** and **4** toward hydrolysis was studied under pseudopharmacological conditions. The hydrolytic decomposition of the compounds was studied in 5 mM NaCl solution

(corresponding to the low intracellular NaCl concentration in cells) and in 100 mM NaCl solution (approximating to the higher NaCl levels in blood plasma). Solutions of the complexes ($c = 2.0$ mM) in aqueous NaCl ($c = 5$ or 100 mM in D_2O containing 10% $[D_6]DMSO$) were prepared and maintained at 37 °C for 7 days. Decomposition of the complexes was monitored by ^{31}P NMR spectroscopy. The curcumin derivative **1** did not undergo hydrolyze in either solution; i.e., the ^{31}P NMR spectrum of **1** remained unchanged in solution after 7 days. In contrast, the bisdemethoxycurcumin derivative **4** immediately underwent partial substitution of the chelating ligand in both 5 and 100 mM aqueous NaCl solution, with two new singlets observed at -34.4 and -30.2 ppm, together with a signal at -27.2 ppm corresponding to the starting cationic species $[Ru(cym)(bdcrc)(PTA)]^+$. After 1 day, the one species observed in the 100 mM aqueous NaCl solution of **4** corresponded to $[Ru(cym)(PTA)Cl_2]$,¹⁷ whereas in the 5 mM aqueous NaCl solution only the starting complex, $[Ru(cym)(bdcrc)(PTA)]^+$, was observed.

The pK_a values of the coordinated PTA ligands in **1** and **4** were determined by ^{31}P NMR spectroscopy in D_2O containing 10% DMSO, by measuring the chemical shift of the complexes at different pD values. The values obtained were plotted as chemical shift vs pD (see Figure 2) and fitted using the

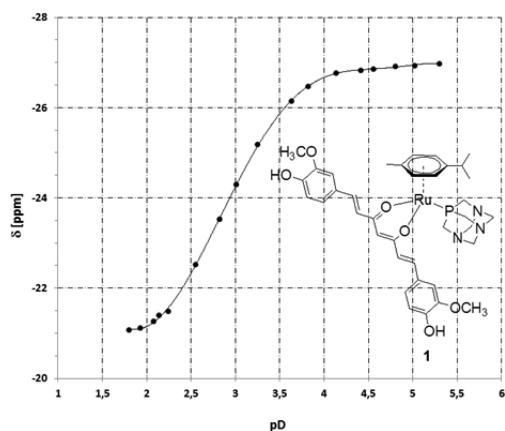


Figure 2. ^{31}P NMR chemical shift vs pD for **1**.

Henderson–Hasselbach equation. The pK_a value is obtained at the midpoint of the curve, with 0.44 being subtracted to account for the difference between the pH and pD.¹⁰

The pK_a values of the free and coordinated ligands are summarized in Table 1. The value for complex **1** is similar to

Table 1. pK_a Values for Complexes **1** and **4** in a 0.1 M NaCl Solution

complex	pK_a
PTA	5.63 ± 0.05
RAPTA-C	3.13 ± 0.02
1	2.41 ± 0.02

those of analogous compounds previously reported^{17,18} and significantly lower than those of RAPTA-C. In contrast, the pK_a determination of coordinated PTA in **4** was not possible, due to the predominant formation of RAPTA-C on lowering the pD with dilute HCl solution. In fact, the measured pK_a corresponds to that previously reported for RAPTA-C.¹⁰

The wavelengths and intensities of the bands in the electronic absorption spectra of the free curcuminoid proligands in DMSO and ethanol are given in Table 2. Each

Table 2. Wavelengths of Maximum Absorbance and Extinction Coefficients for Ligands in DMSO and Ethanol

ligand	DMSO		ethanol		assign
	λ_{max}/nm	$\epsilon/M^{-1} cm^{-1}$	λ_{max}/nm	$\epsilon/M^{-1} cm^{-1}$	
curcH	268	11.155	264	11.167	$n \rightarrow \pi^*$
	448	49.642	431	45.628	$\pi \rightarrow \pi^*$
bdcrcH	264	9.338	252	14.616	$n \rightarrow \pi^*$
	426	53.732	420	53.626	$\pi \rightarrow \pi^*$

free proligand exhibits a $\pi-\pi^*$ transition in the range 420–448 nm, where the maximum absorption is due to allowed $\pi-\pi^*$ type excitations of their extended conjugate systems. The assignment of this transition as $\pi-\pi^*$ was confirmed by solvent effects. When the solvent was changed from ethanol to DMSO, the transition shifted to a longer wavelength. In contrast, $n-\pi^*$ transitions are characteristically shifted to shorter wavelengths with increasing solvent polarity.²⁰

The wavelengths and intensities of the bands in the electronic absorption spectra of the ruthenium complexes containing curc and bdcrc are summarized in Table 3.

Table 3. Wavelengths of Maximum Absorbance and Extinction Coefficients for Ru(II) Arene Complexes Containing Curcuminoid Ligands in DMSO and Ethanol

compd	DMSO		ethanol		assign
	λ_{max}/nm	$\epsilon/M^{-1} cm^{-1}$	λ_{max}/nm	$\epsilon/M^{-1} cm^{-1}$	
1	252	12.367	235	11.936	$n \rightarrow \pi^*$
	430	8.618	427	8.465	$\pi \rightarrow \pi^*$
	481 (sh)	7.060	472 (sh)	6.457	$Ru(4d^6) \rightarrow \pi^*$
2	252	12.283	234	11.851	$n \rightarrow \pi^*$
	430	7.753	430	7.630	$\pi \rightarrow \pi^*$
	483 (sh)	5.745	474 (sh)	6.322	$Ru(4d^6) \rightarrow \pi^*$
3	251	13.227	235	12.811	$n \rightarrow \pi^*$
	430	9.285	427	9.257	$\pi \rightarrow \pi^*$
	480 (sh)	6.656	475 (sh)	7.698	$Ru(4d^6) \rightarrow \pi^*$
4	253	11.487	234	11.603	$n \rightarrow \pi^*$
	417	7.731	413	7.669	$\pi \rightarrow \pi^*$
	480 (sh)	4.153	468 (sh)	5.113	$Ru(4d^6) \rightarrow \pi^*$
5	253	11.467	234	11.318	$n \rightarrow \pi^*$
	417	8.050	415	7.894	$\pi \rightarrow \pi^*$
	479 (sh)	4.763	468 (sh)	5.379	$Ru(4d^6) \rightarrow \pi^*$
6	252	11.893	235	11.893	$n \rightarrow \pi^*$
	419	7.763	415	8.090	$\pi \rightarrow \pi^*$
	478 (sh)	4.930	468 (sh)	5.654	$Ru(4d^6) \rightarrow \pi^*$

All complexes display transitions in the range 450–500 nm as shoulders, assignable to MLCT (metal–ligand charge transfer) from the filled 4d orbitals of Ru(II) to the empty π^* ligand orbitals ($4d^6 Ru \rightarrow \pi^*$)²¹ (Figure 3A,B). The absorption spectra of curcH, bdcrcH, and all ruthenium complexes in both DMSO and ethanol solutions are reported in the Supporting Information (Figure 1S).

The emission spectra of proligands (0.045 mM) and complexes **1**–**6** (0.045 mM) in DMSO (Figure 3C,D) were obtained by irradiation with light of frequencies corresponding to the maximum in their absorption spectra. The proligands are

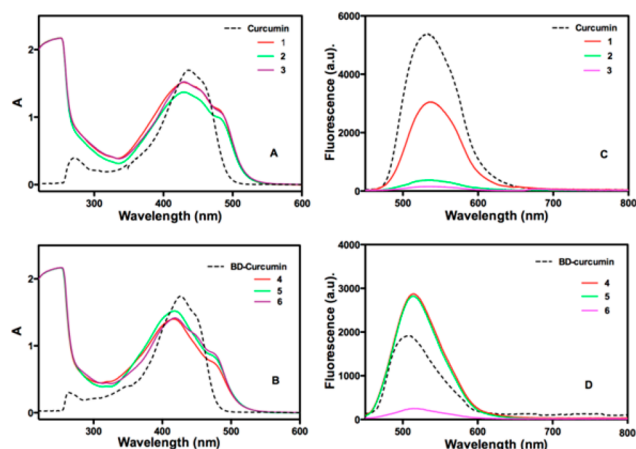


Figure 3. UV-vis spectra of DMSO solutions of (A) curcH and related Ru(II) arene complexes and (B) bdcucurH and related Ru(II) arene complexes. Fluorescence spectra of DMSO solutions of (C) curcH and related Ru(II) arene complexes and (D) bdcucurH and related Ru(II) arene complexes.

fluorescent due to their extended aromatic systems. Complexes 1–3 re-emit at higher wavelengths and lower intensities with respect to the free curcH. In contrast, in the case of the bdcucur Ru(II) complexes, only 6 displays a lowering of intensity, whereas 4 and 5 re-emit with intensities higher than that of the free bdcucurH proligand. The lowest intensities are always obtained with complexes containing the hmb moiety (3 and 6), the six methyl substituents likely being responsible for the deactivation of the emission process. The inversion in the emissive behavior of the cymene complexes 4 and 5 (intensity higher than that of free bdcucurH) with respect to 1 and 2 (lower intensity than free curcH) is due to the absence of methoxy substituents in bdcucurH with respect to the curcH proligand.

The fluorescence data of curcH, bdcucurH, and all ruthenium complexes in DMSO solutions are reported in the Supporting Information (Table 2S).

Biological Studies. The cytotoxicity of 1–6 was evaluated in vitro in comparison to that of cisplatin by determining the IC_{50} concentration against human ovarian carcinoma A2780 cells and the A2780cisR variant with acquired resistance to cisplatin as well as against nontumorous human embryonic kidney (HEK293) cells. IC_{50} values for the compounds determined after 72 h are presented in Table 4.

The new curcumin complexes display a highly promising activity profile. All complexes inhibit the growth of the tumor cell lines at low micromolar concentrations and are more

potent than cisplatin, which is used in the clinic to treat ovarian cancer,²² and curcumin itself (IC_{50} in A2780 and A2780cisR cell lines 8 ± 1 and $11 \pm 2 \mu M$, respectively).²³ Moreover, in all cases the curcumin metal complexes show selectivity toward the tumor cell lines (A2780 and A2780cisR) over the nontumorous HEK293 cell line. In particular, 6 is approximately 70-fold more active against the cancer cell line in comparison to the noncancerous HEK cell line.

Complexes 1–6 are ca. 1–2 orders of magnitude more cytotoxic than [Ru(cym)(curc)Cl] ($23.4 \pm 3.3 \mu M$ on A2780 cells), reported previously,⁷ and related compounds with β -diketonate leaving groups.^{7c,18} RAPTA-C is essentially inactive ($IC_{50} > 250 \mu M$) in the two ovarian cancer cell lines studied.²⁴ Moreover, switching the chloride ligand to the PTA ligand results in complexes that overcome cisplatin resistance. Among the six complexes there is little variation of cytotoxicity in the ovarian cancer cell lines, and replacement of the cymene ligand by the more lipophilic hexamethylbenzene ligand has only a modest impact on the cytotoxic potency of the respective complexes. In addition, switching the curcumin ligand to bisdemethoxycurcumin does not give a straightforward trend. The similar cytotoxicity profiles of the compounds are remarkable given the extreme differences in hydrolysis of the curcumin and bisdemethoxycurcumin ligands, the former being inert and the latter readily dissociating. Thus, at this stage, it is difficult to postulate a mechanism of action, although the cytotoxicity data suggest a common mechanism.

CONCLUSIONS

Curcumin has been extensively used as a food component and has been shown to possess antioxidant, antiproliferative, anticancer, and antiangiogenic properties, and many reports have documented its efficacy in the treatment of a number of diseases.²⁵ Previously reported ruthenium(II)–arene complexes have been reported that show relevant cytotoxic effects toward cancer cells.⁷ Here, we have shown RAPTA-type complexes containing curcumin-based ligands, as potential leaving groups are endowed with not only superior solubility properties but also superior cytotoxicities in comparison to other classes of related compounds. On the cancer cell lines tested these new compounds are ca. 100 fold more cytotoxic, with IC_{50} values being typically $\leq 1 \mu M$, while maintaining an excellent selectivity index: i.e., they are considerably less cytotoxic to nontumorous human embryonic kidney cells. The presence or absence of peripheral methoxy groups in curcumin and the different arene rings do not strongly influence the biological activity, despite leading to differences in hydrolysis rates, whereas the PTA ligand appears to significantly improve the pharmacological properties of the curcumin-modified ruthenium(II)–arene complexes. The superior cytotoxicity and selectivity index in comparison to clinically used cisplatin warrants the further development of these complexes.

EXPERIMENTAL SECTION

Materials and Methods. The dimers [(arene)RuCl₂]₂ (arene = cym, hmb) were purchased from Aldrich. Curcumin and bisdemethoxycurcumin were purchased from TCI Europe and were used as received. All other materials were obtained from commercial sources and were used as received. IR spectra were recorded from 4000 to 600 cm^{-1} on a PerkinElmer Spectrum 100 FT-IR instrument. ¹H and ¹³C NMR spectra were recorded on a 400 Mercury Plus Varian instrument operating at room temperature (400 MHz for ¹H and 100 MHz for ¹³C) relative to TMS. Positive and negative ion electrospray ionization

Table 4. Cytotoxicity (IC_{50} , μM) of 1–6 Following Incubation for 72 h with Nontumorous Human Embryonic Kidney HEK293 Cells and Ovarian Carcinoma A2780 and A2780R (Cisplatin-Resistant) Cell Lines

compd	HEK293	A2780	A2780cisR
1	4.5 ± 0.5	0.39 ± 0.16	0.36 ± 0.02
2	30 ± 1.0	1.15 ± 0.05	1.18 ± 0.02
3	9.1 ± 1.1	0.39 ± 0.01	0.40 ± 0.02
4	22 ± 4.0	0.81 ± 0.14	0.95 ± 0.21
5	2.0 ± 0.1	0.14 ± 0.05	0.51 ± 0.10
6	13 ± 2.0	0.20 ± 0.05	0.27 ± 0.03
cisplatin	7.3 ± 0.6	1.5 ± 0.2	25 ± 3.0

mass spectra (ESI-MS) were obtained on a Series 1100 MSI detector HP spectrometer using methanol as the mobile phase. Solutions (3 mg/mL) analysis were prepared using reagent-grade methanol. Masses and intensities were compared to those calculated using IsoPro Isotopic Abundance Simulator, version 2.1.28. Melting points are uncorrected and were recorded on a STMP3 Stuart scientific instrument and on a capillary apparatus. Samples for microanalysis were dried in vacuo to constant weight (20 °C, ca. 0.1 Torr) and analyzed on a Fisons Instruments 1108 CHNS-O elemental analyzer. Electrical conductivity measurements (Λ_m , reported as S cm² mol⁻¹) of acetonitrile and dichloromethane solutions of the complexes were recorded using a Crison CDTM 522 conductimeter at room temperature. UV-vis spectra of the proligands and complexes were performed with a Varian Cary1 spectrometer at 20 °C. The fluorescence of the proligands and complexes was analyzed using a Hitachi F-4500 spectrofluorimeter at 20 °C.

Synthesis of Ruthenium Complexes. *[Ru(cym)(curc)(PTA)]-[SO₃CF₃]* (**1**). Curcumin (curc, 368 mg, 1.00 mmol) was dissolved in methanol (20 mL), and KOH (56 mg, 1.0 mmol) was added. The mixture was stirred for 1 h at room temperature, and then *[Ru(cymene)Cl₂]₂* (306 mg, 0.50 mmol) was added. The resulting mixture was stirred under reflux for 24 h, and then AgSO₃CF₃ (257 mg, 1 mmol) was added. The reaction mixture was stirred for 1 h and filtered to remove AgCl. PTA (PTA = 1,3,5-triaza-7-phosphaadamantane; 157 mg, 1 mmol) was finally added to the filtrate, which was stirred for 24 h at room temperature. Then, the solvent was removed and the crude product recrystallized from a 3/1 mixture of dichloromethane and *n*-hexane (25 mL) by cooling to 4 °C until an orange crystalline powder formed (491 mg, 0.54 mmol, yield 54%), which was identified as **1**. It is soluble in alcohols, acetone, acetonitrile, and DMSO and slightly soluble in chlorinated solvents. Mp: 156–158 °C. Anal. Calcd for C₃₈H₄₅F₃N₃O₃PRuS: C, 50.22; H, 4.99; N, 4.62. Found: C, 50.02; H, 5.02. IR (cm⁻¹): 2966 w, 1619 sh, 1590 m, 1498 s ν (C=C), 1270 m, 1156 s, 1027 s ν (SO₃CF₃). ¹H NMR (DMSO, 293 K): δ 1.26 (d, 6H, CH₃C₆H₄CH(CH₃)₂), 2.00 (s, 3H, CH₃C₆H₄CH(CH₃)₂), 2.64 (m, 1H, CH₃C₆H₄CH(CH₃)₂), 3.81 (s, 6H, OCH₃ of curc), 4.08 (dd, 6H, PTA), 4.41 (dd, 6H, PTA), 5.78 (s, 1H, C(1)H of curc), 6.03 d, 6.09 d (4H, CH₃C₆H₄CH(CH₃)₂), 6.68 (d, 2H, C(3,3')H of curc), 6.80 (d, 2H, C(10,10')H of curc), 7.04 (d, 2H, C(9,9')H of curc), 7.22 (d, 2H, C(6,6')H of curc), 7.32 (d, 2H, C(4,4')H of curc), 9.63 (s, 2H, OH of curc). ¹³C NMR (DMSO, 293 K): δ 17.0 (CH₃C₆H₄CH(CH₃)₂), 22.4 (CH₃C₆H₄CH(CH₃)₂), 30.7 (CH₃C₆H₄CH(CH₃)₂), 51.2 (PCH₂N, PTA), 56.4 (OCH₃ of curc), 72.4 (NCH₂N, PTA), 88.6, 90.4, 96.7 (CH₃C₆H₄CH(CH₃)₂), 104.1 (C(1,1') of curc), 105.1 (C(6,6') of curc), 111.2 (C(9,9') of curc), 116.4 (C(10,10') of curc), 123.9 (C(5,5') of curc), 127.2 (C(3,3') of curc), 140.4 (C(4,4') of curc), 148.7 (C(7,7') of curc), 149.8 (C(8,8') of curc), 180.3 (C(2,2')=O of curc). ³¹P NMR (DMSO, 293 K): δ -25.8. ESI-MS (+) CH₃OH (*m/z* [relative intensity, %]): 760 [100] *[Ru(cymene)(curc)(PTA)]*⁺, 603 [20] *[Ru(cymene)(curc)]*⁺. Λ_m (CH₃OH, 298 K, 10⁻³ mol/L): 88 S cm² mol⁻¹. Λ_m ((CH₃)₂SO, 298 K, 10⁻³ mol/L): 38 S cm² mol⁻¹.

[Ru(cym)(curc)(PTA)][PF₆] (**2**). The synthesis was performed as for **1** using AgPF₆. **2** is soluble in alcohols, acetone, acetonitrile, and DMSO and slightly soluble in chlorinated solvents. Mp: 170–172 °C. Anal. Calcd for C₃₇H₄₅F₆N₃O₂PRu: C, 49.12; H, 5.01; N, 4.64. Found: C, 48.95; H, 5.05; N, 4.54. IR (cm⁻¹): 1605 sh, 1603 m, 1599 sh, 1497 s ν (C=C), 825 s ν (PF₆). ¹H NMR (DMSO, 293 K): δ 1.25 (d, 6H, CH₃C₆H₄CH(CH₃)₂), 1.99 (s, 3H, CH₃C₆H₄CH(CH₃)₂), 2.63 (m, 1H, CH₃C₆H₄CH(CH₃)₂), 3.81 (s, 6H, OCH₃ of curc), 4.08 (dd, 6H, PTA), 4.40 (dd, 6H, PTA), 5.78 (s, 1H, C(1)H of curc), 6.02d, 6.08d (4H, CH₃C₆H₄CH(CH₃)₂), 6.67 (d, 2H, C(3,3')H of curc), 6.79 (d, 2H, C(10,10')H of curc), 7.03 (d, 2H, C(9,9')H of curc), 7.21 (d, 2H, C(6,6')H of curc), 7.31 (d, 2H, C(4,4')H of curc), 9.62 (s, 2H, OH of curc). ¹³C NMR (DMSO, 293 K): δ 17.0 (CH₃C₆H₄CH(CH₃)₂), 22.4 (CH₃C₆H₄CH(CH₃)₂), 30.7 (CH₃C₆H₄CH(CH₃)₂), 51.2 (PCH₂N, PTA), 56.3 (OCH₃ of curc), 72.3 (N-CH₂-N, PTA), 88.6, 90.3, 96.6 (CH₃C₆H₄CH(CH₃)₂), 104.0 (C(1,1') of curc), 105.0 (C(6,6') of curc), 111.2 (C(9,9') of curc), 116.4 (C(10,10') of curc), 123.9 (C(5,5') of curc), 127.2 (C(3,3') of

curc), 140.4 (C(4,4') of curc), 148.7 (C(7,7') of curc), 149.8 (C(8,8') of curc), 180.3 (C(2,2')=O of curc). ³¹P NMR (DMSO, 293 K): δ -26.0 (s, PTA), -143.1 (sept, PF₆). ESI-MS (+) CH₃OH (*m/z* [relative intensity, %]): 760 [100] *[Ru(cymene)(curc)(PTA)]*⁺, 603 [20] *[Ru(cymene)(curc)]*⁺. Λ_m (CH₃OH, 298 K, 10⁻³ mol/L): 91 S cm² mol⁻¹. Λ_m ((CH₃)₂SO, 298 K, 10⁻³ mol/L): 35 S cm² mol⁻¹.

[Ru(hmb)(curc)(PTA)][SO₃CF₃] (**3**). Compound **3** was prepared following a procedure similar to that reported for **1** by using *[Ru(hmb)Cl₂]₂*. **3** is soluble in alcohols, acetone, acetonitrile, and DMSO and slightly soluble in chlorinated solvents. Mp: 201–203 °C. Anal. Calcd for C₄₀H₄₉F₃N₃O₃PRuS: C, 51.28; H, 5.27; N, 4.48. Found: C, 50.98; H, 5.15; N, 4.36. IR (cm⁻¹): 1619 w, 1590 m, 1498 s ν (C=C), 1273 m, 1157 s, 1028 s ν (SO₃CF₃). ¹H NMR (DMSO, 293 K): δ 2.06 (s, 18H, CH₃(hmb)), 3.82 (s, 6H, PTA), 3.98 (s, 6H, PTA), 4.36 (s, 6H, OCH₃ of curc), 5.78 (s, 1H, C(1)H of curc), 6.74–6.81 (br, 4H, C(3,3')H and C(10,10')H of curc), 7.08 (d, 2H, C(9,9')H of curc), 7.25 (d, 2H, C(6,6')H of curc), 7.43 (d, 2H, C(4,4')H of curc), 9.63 (s, 2H, OH of curc). ¹³C NMR (DMSO, 293 K): δ 15.5 (CH₃(hmb)), 48.8 (PCH₂N, PTA), 56.1 (OCH₃ of curc), 72.1 (NCH₂N, PTA), 97.9 (C₆(hmb)), 104.2 (C(1,1') of curc), 111.2 (C(6,6') of curc), 116.1 (C(9,9') of curc), 123.4 (C(10,10') of curc), 125.0 (C(5,5') of curc), 126.9 (C(3,3') of curc), 139.5 (C(4,4') of curc), 148.4 (C(7,7') of curc), 149.5 (C(8,8') of curc), 179.3 (C(2,2')=O of curc). ³¹P NMR (DMSO, 293 K): δ -32.7. ESI-MS (+) CH₃OH (*m/z* [relative intensity, %]): 788 [100] *[Ru(hmb)(curc)(PTA)]*⁺, 631 [20] *[Ru(hmb)(curc)]*⁺. Λ_m (CH₃OH, 298 K, 10⁻³ mol/L): 97 S cm² mol⁻¹. Λ_m ((CH₃)₂SO, 298 K, 10⁻³ mol/L): 42 S cm² mol⁻¹.

[Ru(cym)(bdcure)(PTA)][SO₃CF₃] (**4**). Compound **4** was prepared following a procedure similar to that reported for **1** by using bdcure. **4** is soluble in alcohols, acetone, acetonitrile, and DMSO and slightly soluble in chlorinated solvents. Mp: 184–186 °C. Anal. Calcd for C₃₆H₄₁F₃N₃O₃PRuS: C, 50.94; H, 4.87; N, 4.95. Found: C, 50.48; H, 4.73; N, 4.68. IR (cm⁻¹): 3261 br, 1620 sh, 1601 m, 1584 sh, ν (C=C), 1269 m, 1155 s, 1025 s ν (SO₃CF₃). ¹H NMR (DMSO, 293 K): δ 1.26 (d, 6H, CH₃C₆H₄CH(CH₃)₂), 1.99 (s, 3H, CH₃C₆H₄CH(CH₃)₂), 2.78 (m, 1H, CH₃C₆H₄CH(CH₃)₂), 4.08 (sbr, 6H, PTA), 4.40 (sbr, 6H, PTA), 5.76 (s, 1H, C(1)H of bdcure), 6.06 (dd, 4H, CH₃C₆H₄CH(CH₃)₂), 6.62 (d, 2H, C(4,4')H of bdcure), 6.79–6.83 (br, 4H, C(6,6')H and C(10,10')H of bdcure), 7.33 (d, 2H, C(3,3')H of bdcure), 7.46–7.55 (br, 4H, C(7,7')H and C(9,9')H of bdcure), 10.01 (sbr, 2H, OH). ¹³C NMR (DMSO, 293 K): δ 16.6 (s, CH₃C₆H₄CH(CH₃)₂), 22.1 (s, CH₃C₆H₄CH(CH₃)₂), 30.3 (s, CH₃C₆H₄CH(CH₃)₂), 50.9 (PCH₂N, PTA), 72.1 (NCH₂N, PTA), 88.3, 90.1, 96.2, 103.6 (s, CH₃C₆H₄CH(CH₃)₂), 104.6 (s, C(1,1') of bdcure), 116.3 (s, C(9,9') and C(7,7') of bdcure), 123.4 (s, C(10,10') and C(6,6') of bdcure), 126.4 (s, C(5,5') of bdcure), 130.4 (s, C(3,3') of bdcure), 139.9 (s, C(4,4') of bdcure), 159.9 (s, C(8,8') of bdcure), 180.0 (s, C(2,2')=O of bdcure). ³¹P NMR (DMSO, 293 K): δ -26.0. ESI-MS (+) CH₃OH (*m/z* [relative intensity, %]): 700 [100] *[Ru(cymene)(bdcure)(PTA)]*⁺, 543 [20] *[Ru(cymene)(bdcure)]*⁺. Λ_m (CH₃OH, 298 K, 10⁻³ mol/L): 91 S cm² mol⁻¹. Λ_m ((CH₃)₂SO, 298 K, 10⁻³ mol/L): 41 S cm² mol⁻¹.

[Ru(cym)(bdcure)(PTA)][PF₆] (**5**). Compound **5** was prepared following a procedure similar to that reported for **2** by using bdcure. **5** is soluble in alcohols, acetone, acetonitrile, and DMSO and slightly soluble in chlorinated solvents. Mp: 182–184 °C. Anal. Calcd for C₃₅H₄₁F₆N₃O₂PRu: C, 49.76; H, 4.89; N, 4.97. Found: C, 49.55; H, 4.69; N, 4.81. IR (cm⁻¹): 1603 sh, 1601 m, 1598 sh, 1498 s ν (C=C), 826 s ν (PF₆). ¹H NMR (DMSO, 298 K): δ 1.25 (d, 6H, CH₃C₆H₄CH(CH₃)₂), 1.99 (s, 3H, CH₃C₆H₄CH(CH₃)₂), 2.77 (m, 1H, CH₃C₆H₄CH(CH₃)₂), 4.07 (sbr, 6H, PTA), 4.40 (sbr, 6H, PTA), 5.76 (s, 1H, C(1)H of bdcure), 6.06 (dd, 4H, CH₃C₆H₄CH(CH₃)₂), 6.62 (d, 2H, C(4,4')H of bdcure), 6.79–6.83 (br, 4H, C(7,7')H and C(9,9')H of bdcure), 7.33 (d, 2H, C(3,3')H of bdcure), 7.48 (br, 4H, C(6,6')H and C(10,10')H of bdcure), 10.02 (sbr, 2H, OH). ¹³C NMR (DMSO, 293 K): δ 16.6 (s, CH₃C₆H₄CH(CH₃)₂), 22.1 (s, CH₃C₆H₄CH(CH₃)₂), 30.3 (s, CH₃C₆H₄CH(CH₃)₂), 50.9 (PCH₂N, PTA), 72.1 (NCH₂N, PTA), 88.3, 90.1, 96.2, 103.6 (s, CH₃C₆H₄CH(CH₃)₂), 104.6 (s, C(1,1') of bdcure), 116.4 (s, C(9,9') and C(7,7') of

bdcurc), 123.5 (s, C(10,10')) and C(6,6') of bdcurc), 126.4 (s, C(5,5') of bdcurc), 130.6 (s, C(3,3') of bdcurc), 139.8 (s, C(4,4') of bdcurc), 159.9 (s, C(8,8') of bdcurc), 180.0 (s, C(2,2')=O of bdcurc). ^{31}P NMR (DMSO, 298 K): δ -26.1 (s, PTA), -143.2 (sept, PF_6). ESI-MS (+) CH_3OH (m/z [relative intensity, %]): 700 [100] $[\text{Ru}(\text{cymene})(\text{bdcurc})(\text{PTA})]^+$, 543 [10] $[\text{Ru}(\text{cymene})(\text{bdcurc})]^+$. Λ_m (CH_3OH , 298 K, 10^{-3} mol/L): 89 $\text{S cm}^2 \text{mol}^{-1}$. Λ_m ($(\text{CH}_3)_2\text{SO}$, 298 K, 10^{-3} mol/L): 44 $\text{S cm}^2 \text{mol}^{-1}$.

[Ru(hmb)(bdcurc)(PTA)][SO₃CF₃] (6). Compound 6 was prepared following a procedure similar to that reported for 3 by using bdcurc. 6 is soluble in alcohols, acetone, acetonitrile, and DMSO and slightly soluble in chlorinated solvents. Mp: 209–211 °C. Anal. Calcd for $\text{C}_{38}\text{H}_{45}\text{F}_3\text{N}_3\text{O}_7\text{PRuS}$: C, 52.05; H, 5.17; N, 4.79. Found: C, 51.92; H, 5.04; N, 4.62. IR (cm^{-1}): 1604 sh, 1601 m, 1598 sh, 1497 s ($\nu(\text{C}=\text{C})$), 1270 m, 1160 s, 1027 s ($\nu(\text{CF}_3\text{SO}_3)$). ^1H NMR (DMSO, 293 K): δ 2.07 (s, 18H, $\text{CH}_{3\text{hmb}}$), 3.97 (s, 6H, PTA), 4.35 (s, 6H, PTA), 5.74 (s, 1H, C(1)H of bdcurc), 6.70 (d, 2H, C(4,4')H of bdcurc), 6.80 (br, 4H, C(7,7')H and C(9,9')H of bdcurc), 7.45 (d, 2H, C(3,3')H of bdcurc), 7.53 (br, 4H, C(6,6')H and C(10,10')H of bdcurc), 10.01 (sbr, 2H, OH). ^{13}C NMR (DMSO, 293 K): δ 15.4 (s, $\text{CH}_{3\text{hmb}}$), 48.8 (s, PCH_2N , PTA), 72.1 (s, NCH_2N , PTA), 98.0 (s, $\text{C}_{6\text{hmb}}$), 104.6 (s, C(1,1') of bdcurc), 116.3 (s, C(9,9') and C(7,7') of bdcurc), 124.4 (s, C(10,10') and C(6,6') of bdcurc), 126.5 (s, C(5,5') of bdcurc), 130.6 (s, C(3,3') of bdcurc), 139.3 (s, C(4,4') of bdcurc), 159.8 (s, C(8,8') of bdcurc), 179.3 (s, C(2,2')=O of bdcurc). ^{31}P NMR (DMSO, 298 K): δ -32.7. ESI-MS (+) CH_3OH (m/z [relative intensity, %]): 728 [80] $[\text{Ru}(\text{hmb})(\text{bdcurc})(\text{PTA})]^+$, 571 [100] $[\text{Ru}(\text{hmb})(\text{bdcurc})]^+$. Λ_m (CH_3OH , 298 K, 10^{-3} mol/L): 95 $\text{S cm}^2 \text{mol}^{-1}$. Λ_m ($(\text{CH}_3)_2\text{SO}$, 298 K, 10^{-3} mol/L): 43 $\text{S cm}^2 \text{mol}^{-1}$.

X-ray Crystallography. The diffraction data of compounds 1 and 6 were measured at low temperature (100(2) K) using Mo $K\alpha$ radiation on a Bruker APEX II CCD diffractometer equipped with a κ geometry goniometer. The data sets were reduced by EvalCCD²⁶ and then corrected for absorption.²⁷ The data collection of compound 3 was carried out at low temperature (140(2) K) using Cu $K\alpha$ radiation on an Agilent Technologies SuperNova dual system in combination with an Atlas CCD detector. The data reduction was carried out by CrysAlis PRO.²⁸ The solutions and refinements were performed with SHELX.²⁹ The crystal structures were refined using full-matrix least squares based on F^2 with all non-hydrogen atoms anisotropically defined. Hydrogen atoms were placed in calculated positions by means of the "riding" model.

Determination of pK_a Values. The pH values of NMR samples in D_2O were measured at 298 K, directly in the NMR tube, using a 713 pH meter (Metrohm) equipped with an electrode calibrated with buffer solutions at pH values of 4, 7, and 9. The pH values were adjusted with dilute HCl and NaOH. The pH titration curves were fitted to the Henderson–Hasselbach equation using the program Matlab (MathWorks Software), with the assumption that the observed chemical shifts are weighted averages according to the populations of the protonated and deprotonated species. The resonance frequencies change smoothly with pH between the chemical shifts of the charged form HA^+ , stable in acidic solution, and those of the neutral, deprotonated form A, which is present at high pH. At any pH, the observed chemical shift is a weighted average of the two extreme values $\delta(\text{HA}^+)$ and $\delta(\text{A})$:

$$\delta_{\text{av}} = \frac{\delta(\text{HA}^+)[\text{HA}^+] + \delta(\text{A})[\text{A}]}{[\text{HA}^+] + [\text{A}]}$$

The midpoint of the titration occurs when the concentrations of the acid and its conjugate base are equal, $[\text{HA}^+] = [\text{A}]$: that is, when the pH equals the pK_a of the compound. The pH at the midpoint of the curve is corrected by subtracting 0.44 to the pD values, since the measurements were made in D_2O .³⁰

Cell Culture and Inhibition of Cell Growth. The human A2780 and A2780cisR ovarian carcinoma and HEK (human embryonic kidney) cells were obtained from the European Collection of Cell Cultures (Salisbury, U.K.). A2780 and A2780cisR cells were grown routinely in RPMI-1640 medium, while HEK cells were grown in

DMEM medium, with 10% fetal bovine serum (FBS) and 1% antibiotics at 37 °C and 5% CO_2 . Cytotoxicity was determined using the MTT assay (MTT = 3-(4,5-dimethyl-2-thiazolyl)-2,5-diphenyl-2H-tetrazolium bromide). Cells were seeded in 96-well plates as monolayers with 100 μL of cell suspension (approximately 5000 cells) per well and preincubated for 24 h in medium supplemented with 10% FBS. Compounds were prepared as DMSO solutions and then dissolved in the culture medium and serially diluted to the appropriate concentration, to give a final DMSO concentration of 0.5%. A 100 μL portion of the solution was added to each well, and the plates were incubated for another 72 h. Subsequently, MTT (5 mg/mL solution) was added to the cells and the plates were incubated for a further 2 h. The culture medium was aspirated, and the purple formazan crystals formed by the mitochondrial dehydrogenase activity of vital cells were dissolved in DMSO. The optical density, directly proportional to the number of surviving cells, was quantified at 590 nm using a multiwell plate reader, and the fraction of surviving cells was calculated from the absorbance of untreated control cells. Evaluation is based on means from at least two independent experiments, each comprising triplicates per concentration level.

■ ASSOCIATED CONTENT

● Supporting Information

Tables, figures, and CIF files giving crystallographic data for 1, 3, and 6, absorbances of curcH, bdcurcH, and related Ru(II) arene complexes in DMSO and ethanol, and wavelengths of fluorescence emission maxima of curcH, bdcurcH, and related Ru(II) arene complexes in DMSO. This material is available free of charge via the Internet at <http://pubs.acs.org>.

■ AUTHOR INFORMATION

Corresponding Author

*R.P.: e-mail, riccardo.pettinari@unicam.it; tel, +39 0737402338.

Author Contributions

The manuscript was written through contributions of all authors. All authors have given approval to the final version of the manuscript.

Notes

The authors declare no competing financial interest.

■ ACKNOWLEDGMENTS

We thank the Swiss National Science Foundation (CMM) and the University of Camerino for financial support. We gratefully acknowledge Prof. Renato De Leone (University of Camerino) for the determination of pK_a values by using the program Matlab.

■ REFERENCES

- (a) Wheate, N. J.; Walker, S.; Craig, G. E.; Oun, R. *Dalton Trans.* **2010**, 39, 8113–8127. (b) Jakupec, M. A.; Galanski, M.; Arion, V. B.; Hartinger, C. G.; Keppler, B. K. *Dalton Trans.* **2008**, 183–194.
- (a) Barry, N. P. E.; Sadler, P. J. *Chem. Commun.* **2013**, 49, 5106–5131. (b) Noffke, A. L.; Habtemariam, A.; Pizarro, A. M.; Sadler, P. J. *Chem. Commun.* **2012**, 48, 5219–5246. (c) Gasser, G.; Ott, I.; Metzler-Nolte, N. *J. Med. Chem.* **2011**, 54, 3–25.
- (a) Hartinger, C. G.; Jakupec, M. A.; Zorbas-Seifried, S.; Groessl, M.; Egger, A.; Berger, W.; Zorbas, H.; Dyson, P. J.; Keppler, B. K. *Chem. Biodiversity* **2008**, 5, 2140–2155. (b) Hartinger, C. G.; Zorbas-Seifried, S.; Jakupec, M. A.; Kynast, B.; Zorbas, H.; Keppler, B. K. *Inorg. Biochem.* **2006**, 100, 891–904. (c) Rademaker-Lakhai, J. M.; Van Den Bongard, D.; Pluim, D.; Beijnen, J. H.; Schellens, J. H. M. *Clin. Cancer Res.* **2004**, 10, 3717–3727. (d) Sava, G.; Zorzet, S.; Turrin, C.; Vita, F.; Soranzo, M. R.; Cocchiello, M.; Bergamo, A.; Di Giovine, S.; Pezzoni, G.; Sartor, L.; Garbisa, S. *Clin. Cancer Res.* **2003**, 9, 1898–

1905. (e) Sava, G.; Gagliardi, R.; Bergamo, A.; Alessio, E.; Mestroni, G. *Anticancer Res.* **1999**, *19*, 969–972.
- (4) (a) Hartinger, C. G.; Metzler-Nolte, N.; Dyson, P. J. *Organometallics* **2012**, *31*, 5677–5685. (b) Bergamo, A.; Gaiddon, C.; Schellens, J. H. M.; Beijnen, J. H.; Sava, G. *J. Inorg. Biochem.* **2012**, *106*, 90–99. (c) Smith, G. S.; Therrien, B. *Dalton Trans.* **2011**, *40*, 10793–10800. (d) Ang, W. H.; Casini, A.; Sava, G.; Dyson, P. J. *J. Organomet. Chem.* **2011**, *696*, 989–998. (e) Suss-Fink, G. *Dalton Trans.* **2010**, *39*, 1673–1688. (f) Hartinger, C. G.; Dyson, P. J. *Chem. Soc. Rev.* **2009**, *38*, 391–401. (g) Peacock, A. F. A.; Sadler, P. J. *Chem. Asian J.* **2008**, *3*, 1890–1899.
- (5) For selected examples see: (a) Ang, W. H.; Parker, L. J.; De Luca, A.; Juillerat-Jeanneret, L.; Morton, C. J.; Lo Bello, M.; Parker, M. W.; Dyson, P. J. *Angew. Chem., Int. Ed.* **2009**, *48*, 3854–3857. (b) Kilpin, K. J.; Clavel, C. M.; Edafe, F.; Dyson, P. J. *Organometallics* **2012**, *31*, 7031–7039.
- (6) (a) Ang, W. H.; De Luca, A.; Chapuis-Bernasconi, C.; Juillerat-Jeanneret, L.; Lo Bello, M.; Dyson, P. J. *ChemMedChem* **2007**, *2*, 1799–1806. (b) Kljun, J.; Bytsek, A. K.; Kandiolle, W.; Bartel, C.; Jakupec, M. A.; Hartinger, C. G.; Keppler, B. K.; Turel, I. *Organometallics* **2011**, *30*, 2506–2512. (c) Hudej, R.; Kljun, J.; Kandiolle, W.; Repnik, U.; Turk, B.; Hartinger, C. G.; Keppler, B. K.; Miklavcic, D.; Turel, I. *Organometallics* **2012**, *31*, 5867–5874. (d) Filak, L. K.; Mühlgassner, G.; Bacher, F.; Roller, A.; Galanski, M.; Jakupec, M. A.; Keppler, B. K.; Arion, V. B. *Organometallics* **2011**, *30*, 273–283. (e) Filak, L. K.; Goschl, S.; Hackl, S.; Jakupec, M. A.; Arion, V. B. *Inorg. Chem.* **2012**, *393*, 252–260. (f) Nazarov, A. A.; Gardini, D.; Baquie, M.; Juillerat-Jeanneret, L.; Serkova, T. P.; Shevtsova, E. P.; Scopelliti, R.; Dyson, P. J. *Dalton Trans.* **2013**, *42*, 2347–2350. (g) Filak, L. K.; Goschl, S.; Heffeter, P.; Samper, K. G.; Egger, A. E.; Jakupec, M. A.; Keppler, B. K.; Berger, W.; Arion, V. B. *Organometallics* **2013**, *32*, 903–914.
- (7) (a) Caruso, F.; Rossi, M.; Benson, A.; Opazo, C.; Freedman, D.; Monti, E.; Gariboldi, M. B.; Shaulky, J.; Marchetti, F.; Pettinari, R.; Pettinari, C. *J. Med. Chem.* **2012**, *55*, 1072–1081. (b) Bonfili, L.; Pettinari, R.; Cuccioloni, M.; Cecarini, V.; Mozzicafreddo, M.; Angeletti, M.; Lupidi, G.; Marchetti, F.; Pettinari, C.; Eleuteri, A. M. *ChemMedChem* **2012**, *7*, 2010–2020. (c) Aliende, C.; Pérez-Manrique, M.; Jalón, F. A.; Manzano, B. R.; Rodríguez, A. M.; Cuevas, J. V.; Espino, G.; Martínez, M. Á.; Massaguer, A.; González-Bártulos, M.; de Llorens, R.; Moreno, V. J. *Inorg. Biochem.* **2012**, *117*, 171–188.
- (8) (a) Aggarwal, B. B.; Sundaram, C.; Malani, N.; Ichikawa, H. *Curcumin: The Indian solid gold*; Springer: New York, 2007. (b) Yang, F.; Lim, P. L. G. P.; Begum, A. N.; Ubeda, O. J.; Simmons, M. R.; Ambegaokar, S. S.; Chen, P.; Kaye, R.; Glabe, C. G.; Frautsch, S. A. Cole, G. M. *J. Biol. Chem.* **2004**, *280*, 5892–5901. (c) Aggarwal, B. B.; Kumar, A.; Bharti, A. C. *Anticancer Res.* **2003**, *23*, 363–398.
- (9) For selected examples see: (a) Renfrew, A. K.; Bryce, N. S.; Hambley, T. W. *Chem. Sci.* **2013**, *4*, 3731–3739. (b) Banerjee, S.; Prasad, P.; Hussain, A.; Khan, I.; Kondaiah, P.; Chakravarty, A. R. *Chem. Commun.* **2012**, *48*, 7702–7704. (c) Sagnou, M.; Benaki, D.; Triantis, C.; Tsotakos, T.; Psycharis, V.; Raptopoulou, C. P.; Pirmettis, I.; Papadopoulos, M.; Pelecanou, M. *Inorg. Chem.* **2011**, *50*, 1295–1303. (d) Song, X. Y.-M.; Xu, J.-P.; Ding, L.; Hou, Q.; Liu, J.-W.; Zhu, Z.-L. *J. Inorg. Biochem.* **2009**, *103*, 396–400. (e) Ferrari, E.; Lazzari, S.; Marverti, G.; Pignedoli, F.; Spagnolo, F.; Saladini, M. *Bioorg. Med. Chem.* **2009**, *17*, 3043–3052. (f) Valentini, A.; Conforti, F.; Crispini, A.; De Martino, A.; Condello, R.; Stelitano, C.; Rotilio, G.; Ghedini, M.; Federici, G.; Bernardini, S.; Pucci, D. *J. Med. Chem.* **2009**, *52*, 484–491. (g) Mohammadi, K.; Thompson, K. H.; Patrick, B. O.; Storr, T.; Martins, C.; Polishchuk, E.; Yuen, V. G.; McNeill, J. H.; Orvig, C. *J. Inorg. Biochem.* **2005**, *99*, 2217–2225.
- (10) Scolaro, C.; Bergamo, A.; Brescacin, L.; Delfino, R.; Cocchietto, M.; Laurenczy, G.; Geldbach, T. J.; Sava, G.; Dyson, P. J. *J. Med. Chem.* **2005**, *48*, 4161–4171.
- (11) Nowak-Sliwinska, P.; van Beijnum, J. R.; Casini, A.; Nazarov, A. A.; Wagnieres, G.; van den Bergh, H.; Dyson, P. J.; Griffioen, A. W. *J. Med. Chem.* **2011**, *54*, 3895–3902.
- (12) Chatterjee, S.; Kundu, S.; Bhattacharyya, A.; Hartinger, C. G.; Dyson, P. J. *J. Biol. Inorg. Chem.* **2008**, *13*, 1149–1155.
- (13) (a) Kruck, T. *Angew. Chem., Int. Ed.* **1967**, *6*, 53–67. (b) Collong, W.; Kruck, T. *Chem. Ber.* **1990**, *123*, 1655–1656. (c) Fuss, W.; Ruhe, M. *Z. Naturforsch., B* **1992**, *47B*, 1.
- (14) Nakamoto, K. *Infrared and Raman Spectra of Inorganic and Coordination Compounds*, 5th ed.; Wiley: New York, 1997; Part B, Vol. I-3, p 79.
- (15) Wanke, R.; Smolenski, P.; Guedes da Silva, M. F. C.; Martins, L. M. D. R. S.; Pombeiro, A. J. L. *Inorg. Chem.* **2008**, *47*, 10158–10168.
- (16) Kilpin, K. J.; Clavel, C. M.; Edafe, F.; Dyson, P. J. *Organometallics* **2012**, *31*, 7031–7039.
- (17) Ang, W. H.; Daldini, E.; Scolaro, C.; Scopelliti, R.; Juillerat-Jeanneret, L.; Dyson, P. J. *Inorg. Chem.* **2006**, *45*, 9006–9013.
- (18) Vock, C. A.; Renfrew, A. K.; Scopelliti, R.; Juillerat-Jeanneret, L.; Dyson, P. J. *Eur. J. Inorg. Chem.* **2008**, 1661–1671.
- (19) Allardyce, C. S.; Dyson, P. J.; Ellis, D. J.; Heath, S. L. *Chem. Commun.* **2001**, 1396–1397.
- (20) Lambert, J. B.; Shurvell, H. F.; Lightner, D. A.; Cooks, R. G. *Organic Structural Spectroscopy*; Prentice Hall: New York, 1998.
- (21) Dougan, S. J.; Melchart, M.; Habtemariam, A.; Parsons, S.; Sadler, P. J. *Inorg. Chem.* **2006**, *45*, 10882–10894.
- (22) Wheate, N. J.; Walker, S.; Craig, G. E.; Ouna, R. *Dalton Trans.* **2010**, *39*, 8113–8127.
- (23) Ferrari, E.; Pignedoli, F.; Imbriano, C.; Marverti, G.; Basile, V.; Venturi, E.; Saladini, M. *J. Med. Chem.* **2011**, *54*, 8066–8077.
- (24) Adhikarsan, Z.; Davey, G. E.; Campomanes, P. R.; Groessl, M.; Clavel, C.; Yu, H.; Nazarov, A. A.; Yeo, C. H. F.; Ang, W. H.; Dröge, P.; Roethlisberger, U.; Dyson, P. J.; Davey, C. A. *Nat. Commun.* **2014**, *5*, 3462.
- (25) (a) Shishodia, S.; Chaturvedi, M. M.; Aggarwal, B. B. *Curr. Problems Cancer* **2007**, *31*, 243–305. (b) Agrawal, D. K.; Mishra, P. K. *Med. Res. Rev.* **2010**, *30*, 818–860. (c) Rahman, I.; Biswas, S. K.; Kirkham, P. A. *Biochem. Pharmacol.* **2006**, *72*, 1439–1452.
- (26) Duisenberg, A. J. M.; Kroon-Batenburg, L. M. J.; Schreurs, A. M. *J. Appl. Crystallogr.* **2003**, *36*, 220–229.
- (27) Blessing, R. H. *Acta Crystallogr., Sect. A* **1995**, *51*, 33–38.
- (28) *Crysalis PRO*, release 1.171.37.31; Agilent Technologies, Santa Clara, CA, 2014.
- (29) SHELX: Sheldrick, G. M. *Acta Crystallogr., Sect. A* **2008**, *64*, 112–122.
- (30) Mikkelsen, K.; Nielsen, S. O. *J. Phys. Chem.* **1960**, *64*, 632–637.